PRS-220, a novel inhalable therapeutic intervention for IPF, targeting CTGF directly in the lung

Vanessa Neiens, Marina Pavlidou, Claudia Wurzenberger, Eva-Maria Hansbauer, Cornelia Wurzenberger, Stefan Grüner, Theresia Mosebach, Marleen Richter, Janet Peper-Gabriel, Kristina Heinig, Thomas Jaquin, Antonio Konitsiotis, Josefine Morgenstern, Gabriele Matschiner and Shane Olwill

Pieris Pharmaceuticals GmbH, Zeppelinstrasse 3, 85399 Hallbergmoos - Germany

Idiopathic pulmonary fibrosis (IPF) is a chronic, progressive, and ultimately fatal lung disease characterized by progressive scarring of interstitial lung tissue. The unmet medical need for well-tolerated and effective therapies is very high due to the poor prognosis for patients and limited benefits conferred by current standard of care.

CTGF/CCN2, a matricellular protein highly abundant in IPF tissues (Pan et al., Eur Resp J 2001 and Figure 1) and driver of fibrotic lung remodeling, has been validated as a novel intervention point for IPF treatment in recent clinical trials with the systemically delivered monoclonal antibody pamrevlumab (Richeldi et al., Lancet Respir Med 2019).

Delivery of a CTGF inhibitor directly to the lung via oral inhalation is expected to be advantageous compared to systemically administered antibodies for the following reasons:

- Enhanced drug exposure and local target engagement in the lung
- Better target saturation due to avoidance of systemic CTGF sink
- Pulmonary administration providing greater convenience for patients

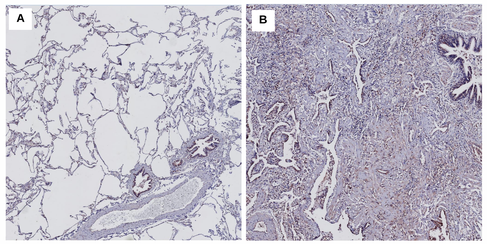

Figure 1. CTGF immunohistochemistry of A) human control and B) IPF lung tissues (collaboration with Prof. Dr. Janette Burgess, University of Groningen, Netherlands).

Anticalin® proteins are a novel class of biotherapeutics which – based on their biophysical properties & small size of approximately 20 kDa – are particularly well-suited for delivery via inhalation (Figure 2).

Here, we describe the preclinical profile of PRS-220, an Anticalin protein targeting CTGF, as a novel and promising inhaled therapy for IPF.

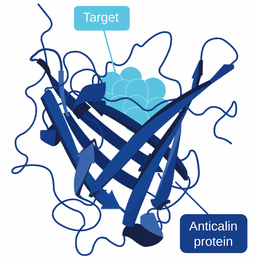

- **Human** – Scaffold derived from human lipocalins (extracellular binding proteins)
- **Specific** – High potency and selectivity for targets
- **Small** – Monomeric, monovalent, small size (~20 kDa vs ~150 kDa mAbs)
- **Stable** – High melting temperatures & insensitivity to mechanical stress
- **Formulable** – Nebulization & dry powder inhalation
- **Proprietary** – Broad IP position on platform and derived products
- **Validated** – Strong industrial partners and clinically tested

Favorable drug-like properties for lung delivery

Figure 2. Schematic representation of an Anticalin protein and characteristics supporting their favorable profile for lung delivery.

PRS-220 binds to the active epitope of CTGF with superior binding properties as pamrevlumab

- **PRS-220 binds CTGF with high affinity (in the picomolar range) and retains a more stable target engagement when compared to the anti-CTGF antibody pamrevlumab.**
- **PRS-220 shares an overlapping epitope with pamrevlumab and effectively displaces the antibody from CTGF with a 5-fold lower IC_{50}.**
- **PRS-220 binds in a dose-dependent manner to CTGF endogenously expressed by TGF-β1 activated NHLF.**

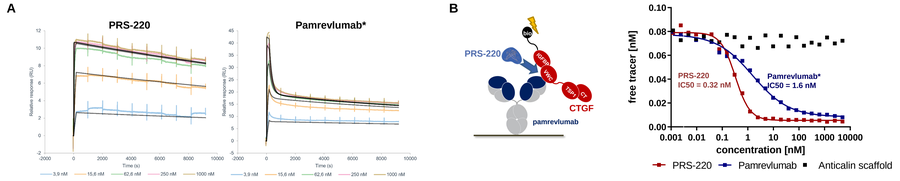

Compound	Fit	kon [M-1*s-1]	koff [s-1]	KD [nM]	kon2 [RU-1*s-1]	koff2 [s-1]	KD2 [M]
PRS-220	1:1 binding	4.06E+05	2.78E-05	0.068			
Pamrevlumab*	Bivalent analyte	1.83E+05	2.74E-03	14.972	4.18E-04	4.17E-05	0.100

** Pamrevlumab was generated in-house from patent signatures.*

Figure 3. Binding properties of PRS-220 in comparison to pamrevlumab. A) Surface Plasmon Resonance (SPR) binding experiment showing the binding of PRS-220 (left) and pamrevlumab (right) to CTGF. **B)** Competition of PRS-220 with pamrevlumab for binding to CTGF and competition of pamrevlumab with itself for binding to CTGF by ELISA. **C)** Dose-dependent binding of PRS-220 to CTGF expressed by disease-relevant TGF-β1 activated primary normal human lung fibroblasts (NHLF) detected by immunofluorescence staining for the PRS-220 scaffold. Pamrevlumab was generated in-house from patent signatures.

PRS-220 achieves superior exposure in the lung

- **Pharmacokinetic analysis of PRS-220 upon lung delivery confirms significant pulmonary exposure over 24 h.**
- **PRS-220 achieves high exposure in the lung while only ~ 1 % reaches the circulation.**
- **In comparison, pulmonary exposure of the systemically delivered pamrevlumab is significantly lower in BALF and lung tissue with only ~ 20 % reaching the lung tissue.**

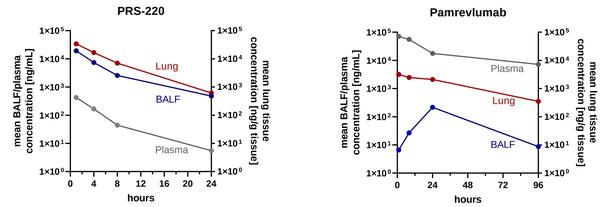

	Lung exposure compared to plasma (%)	Plasma exposure compared to lung (%)
PRS-220	100*	0.9
Pamrevlumab	20.3	100*

** Exposure was set to 100% for compartment of administration.*

Figure 4. Comparison of PRS-220 and pamrevlumab pharmacokinetic (PK) profile in mice. PK analysis of PRS-220 delivered to the lung and pamrevlumab given intravenously (both 100 µg/mouse) in bronchoalveolar lavage fluid (BALF), lung tissue & plasma of mice. Total drug levels were determined by ELISA. Table shows comparison of lung and plasma exposure determined by non-compartmental analysis (NCA). Pamrevlumab was generated in-house from patent signatures.

PRS-220 penetrates fibrotic tissue *in vivo*

- **PRS-220 reveals favorable tissue distribution profile upon delivery to fibrotic lungs of bleomycin-challenged mice.**
- **PRS-220 is not only detected in the airways but also penetrates the fibrotic, interstitial lung tissue.**

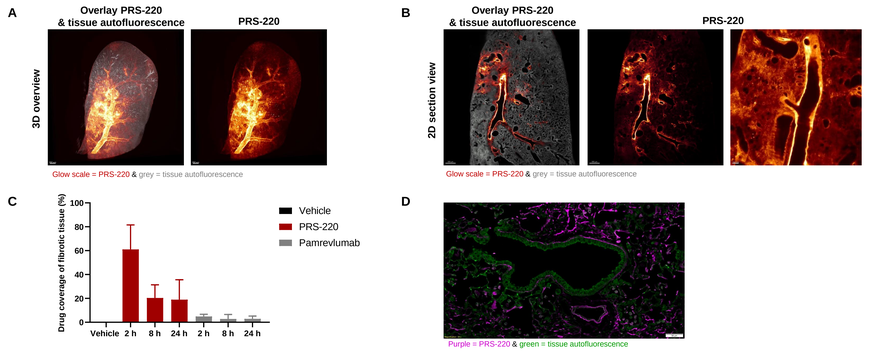

Figure 5. Lung biodistribution of PRS-220 upon delivery to fibrotic lungs of mice. Alexa-647 labeled PRS-220 (100 µg/mouse) delivered to lungs of bleomycin challenged mice (d21) was imaged by light sheet microscopy. **A)** 3D overview of PRS-220 in whole left lung 2 h after dosing (scale bars 500 µm). **B)** Magnified 2D sections from 3D scanned lung (scale bars 500 µm ≙150 µm) shown in A). **C)** Compound accumulation of PRS-220 delivered to the lung and pamrevlumab administered intravenously (both 100 µg/mouse) in fibrotic tissue determined by light sheet imaging & quantitative analysis (n = 2-5 per group). **D)** 2D histological analysis of PRS-220 in lung tissue sections 2 h after delivery to fibrotic mouse lungs. All images are representative for imaging of n=3-6 lungs. PRS-220 was imaged at 630 nm excitation channel and tissue autofluorescence at 560 nm.

PRS-220 is suitable for pulmonary delivery using a nebulizer

- **Favorable biophysical properties allow PRS-220 to retain stability and integrity upon nebulization.**
- **Aerosols generated using vibrating mesh technology show aerodynamic properties suitable for effective lung deposition.**
- **Multiple devices show favorable treatment time, aerodynamic properties and deposited dose.**

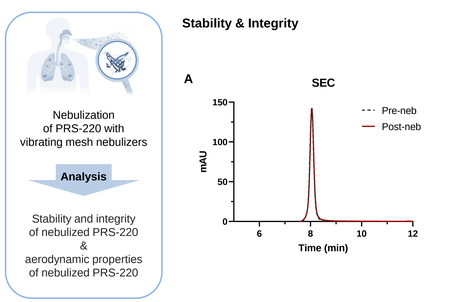

B

PRS-220 aerosol delivery performance		
Laser diffraction	**Droplet size (VMD)**	3.0 µm
	FPF (LD)	89.3 %
NGI	**MMAD**	3.8 µM
	FPF (NGI)	74.5 %
Breathing simulator	**Delivered Dose**	57.7 %
	Nebulization time (1.2 mL)	02:47 min

VMD: Volumetric mean diameter
LD: Laser diffraction
FPF: Fine particle fraction
NGI: Next Generation Cascade Impactor
MMAD: Mass median aerodynamic diameter

Figure 6. *In vitro* nebulization performance of PRS-220 with exemplary vibrating mesh devices. PRS-220 was nebulized by vibrating mesh nebulizers at a concentration of 50 mg/mL and with a filling volume of 1.2 mL for all measurements. **A)** Size exclusion chromatography (SEC) analyzing PRS-220 integrity pre and post nebulization. **B)** Assessment of PRS-220 aerosol delivery performance parameters by laser diffraction, breathing simulator & Next Generation Cascade Impactor analysis. The particle size distribution varies depending on test set-up (temperature, humidity, etc.), explaining the slight difference between NGI and LD particle size measurements.

Inhaled delivery of PRS-220 in rats confirms favorable PK profile for lung delivery

- **The pharmacokinetic profile of PRS-220 was investigated as part of the preclinical toxicology assessment in rats.**
- **Inhaled delivery of PRS-220 in rats achieves high lung levels with low systemic exposure. PK profile of inhaled delivery in rodents supports 1-2x daily dosing.**
- **No adverse findings were observed in this 4-day dose-range finding inhalation study. PRS-220 was well-tolerated up to a dose level of 57 mg/kg/day.**

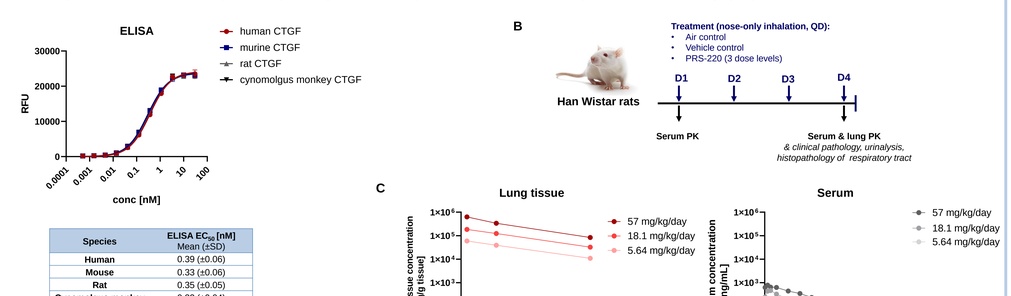

Species	ELISA EC_{50} [nM] Mean (±SD)
Human	0.39 (±0.06)
Mouse	0.33 (±0.06)
Rat	0.35 (±0.05)
Cynomolgus monkey	0.32 (±0.04)

Figure 7. PRS-220 pharmacokinetic profile upon inhaled administration to rats. **A)** Binding of PRS-220 to CTGF from human, mouse, rat and cynomolgus monkey measured by ELISA confirms cross-reactivity of PRS-220 to CTGF from different species. **B)** Design of preclinical toxicology study in rats with daily delivery of PRS-220 at 3 different dose levels by nose-only inhalation for 4 days. **C)** PK profile of inhaled PRS-220 at day 4 including analysis of total drug levels in the lung and free drug levels in serum measured by an electrochemiluminescence assay (ECLA). Figure legend indicates combined mean achieved delivered dose levels assessed at day 1 and day 4 of the study.

Conclusions

- **PRS-220 is an Anticalin-based biotherapeutic for the treatment of IPF designed for inhaled delivery via the nebulized route of administration.**
- **PRS-220 targets the functionally active epitope of CTGF with high affinity and shows more stable target engagement than the clinically active antibody pamrevlumab.**
- **PRS-220 is suitable for inhaled administration using a vibrating mesh nebulizer.**
- **PK and lung biodistribution behavior in rodents supports beneficial profile for lung delivery.**

PRS-220's preclinical profile supports progressing to clinical development with a planned start of Phase 1 studies in 2022. In addition to IPF, PRS-220 will be explored for the treatment of post-acute sequelae of SARS-CoV-2 infection (PASC) pulmonary fibrosis (PASC-PF), also known as post-COVID-19 syndrome pulmonary fibrosis.

ACKNOWLEDGEMENTS - We would like to especially thank the scientists and research assistants who performed these experiments or provided important pre-work to the presented experiments: Alexander Hahn, Mareike Maurer, Christina Grasmüller, Nicolas Quilitz, Sarah Schmalbrock, David Goricanec, Patrick Zägel and Adam Cichy.

AUTHORS RELEVANT INTERESTS – All authors are employees of Pieris Pharmaceuticals and hold stock or stock options in Pieris Pharmaceuticals, Inc.

FUNDING - This work is partially funded by a grant from the Bavarian Ministry of Economic Affairs, Regional Development and Energy within the framework of the Bavarian Therapy Strategy to combat the COVID-19 pandemic ("BayTherapie2020").

Sponsored by
Bavarian Ministry of Economic Affairs, Regional Development and Energy